

**Toward Practical Gas Sensing with Highly Reduced Graphene Oxide: A New Signal Processing  
Method to Circumvent Run-to-Run and Device-to-Device Variations**

Ganhua Lu<sup>1</sup>, Sungjin Park<sup>2</sup>, Kehan Yu<sup>1</sup>, Rodney S. Ruoff<sup>2</sup>, Leonidas E. Ocola<sup>3</sup>, Daniel Rosenmann<sup>3</sup>,  
and Junhong Chen<sup>1\*</sup>

<sup>1</sup> Department of Mechanical Engineering, University of Wisconsin-Milwaukee  
3200 North Cramer Street, Milwaukee, Wisconsin 53211, USA

<sup>2</sup> Department of Mechanical Engineering and the Texas Materials Institute, University of Texas at  
Austin  
204 East Dean Keeton, Austin, Texas 78712, USA

<sup>3</sup> Center for Nanoscale Materials, Argonne National Laboratory  
9700 South Cass Ave, Argonne, Illinois 60439, USA

---

\* To whom all correspondence should be addressed. E-mail: [jhchen@uwm.edu](mailto:jhchen@uwm.edu).

## 1. Measurement of contact resistance between R-GO and Au electrode

We used four Au contact pads (#1, #2, #3, and #4) which were partially covered and connected by highly reduced graphene oxide (R-GO) to evaluate the contact resistance between R-GO and Au. Figure S1a is an SEM image of the four Au contact pads which were mostly rectangular (about  $2 \times 0.8$  mm) and separated by  $\sim 0.2$  mm. Each of the pads was partially covered with R-GO; the uncovered area on each contact pad was used for probe connection during electrical measurements. Two terminal  $I_{ds}$ - $V_{ds}$  measurements were carried out between pad pairs of 1-2, 2-3, 1-3, 3-4, and 2-4. The  $I_{ds}$ - $V_{ds}$  curves in Figure S1b are linear and symmetric, implying most likely Ohmic contact between R-GO and Au. The resistance between a contact pad pair was extracted from the slope of the corresponding  $I_{ds}$ - $V_{ds}$  curve. The measured resistance between a contact pad pair could be regarded as the sum of two contact resistances and the resistance of R-GO between these two pads. Thus, the resistance between pads #1 and 2 ( $R_{12}$ ) can be expressed as

$$R_{12} = R_{C1} + R_{G12} + R_{C2}, \quad (S1)$$

where  $R_{C1}$  and  $R_{C2}$  are the contact resistances at pads #1 and 2, respectively, and  $R_{G12}$  is the resistance of R-GO between pads # 1 and #2. Similarly, we can have

$$R_{23} = R_{C2} + R_{G23} + R_{C3} \quad (S2)$$

$$R_{13} = R_{C1} + R_{G13} + R_{C3} \quad (S3)$$

Note that  $R_{G13} = R_{G12} + R_{G23}$  since the R-GO in contact with pad #2 was short-circuited by Au during  $I_{ds}$ - $V_{ds}$  measurement for pads # 1 and 3. Hence, combining (S1), (S2), and (S3) yields

$$R_{C2} = (R_{12} + R_{23} - R_{13})/2. \quad (S4)$$

Likewise, we can have the contact resistance for pad #3 as

$$R_{C3} = (R_{23} + R_{34} - R_{24})/2. \quad (S5)$$

For the device before  $NO_2$  exposure, we obtained  $R_{12} = \sim 1,860$  k $\Omega$ ,  $R_{23} = \sim 626$  k $\Omega$ ,  $R_{13} = \sim 2,384$  k $\Omega$ ,  $R_{34} = \sim 598$  k $\Omega$ , and  $R_{24} = \sim 1,204$  k $\Omega$  using  $I_{ds}$ - $V_{ds}$  curves (solid ones) in Figure S1b and got  $R_{C2} \sim$

50 k $\Omega$  and  $R_{C3} \sim 10$  k $\Omega$  using equations (S4) and (S5). Therefore, the contact resistance between pads # 2 and 3 is  $\sim 10\%$  of the total resistance, or  $(R_{C2}+R_{C3})/R_{23} \sim 10\%$ .

In addition, Figure S1c shows that the resistance between a pair of Au contact pads (connected by R-GO) increases quite linearly with the increasing gap distance between Au pads, implying that the measured resistances are dominated by the resistance of R-GO rather than the contact resistance between R-GO and the Au contact pads. Of course, the configuration of the four contact pads is quite different from that of the interdigitated electrodes used for R-GO sensors. Nevertheless, the results of our preliminary measurements suggest that the contact between R-GO and Au played a minor role in the total device resistance. More sophisticated measurements on better designed electrode layouts are needed to further investigate the contact issue between R-GO and metal electrodes.

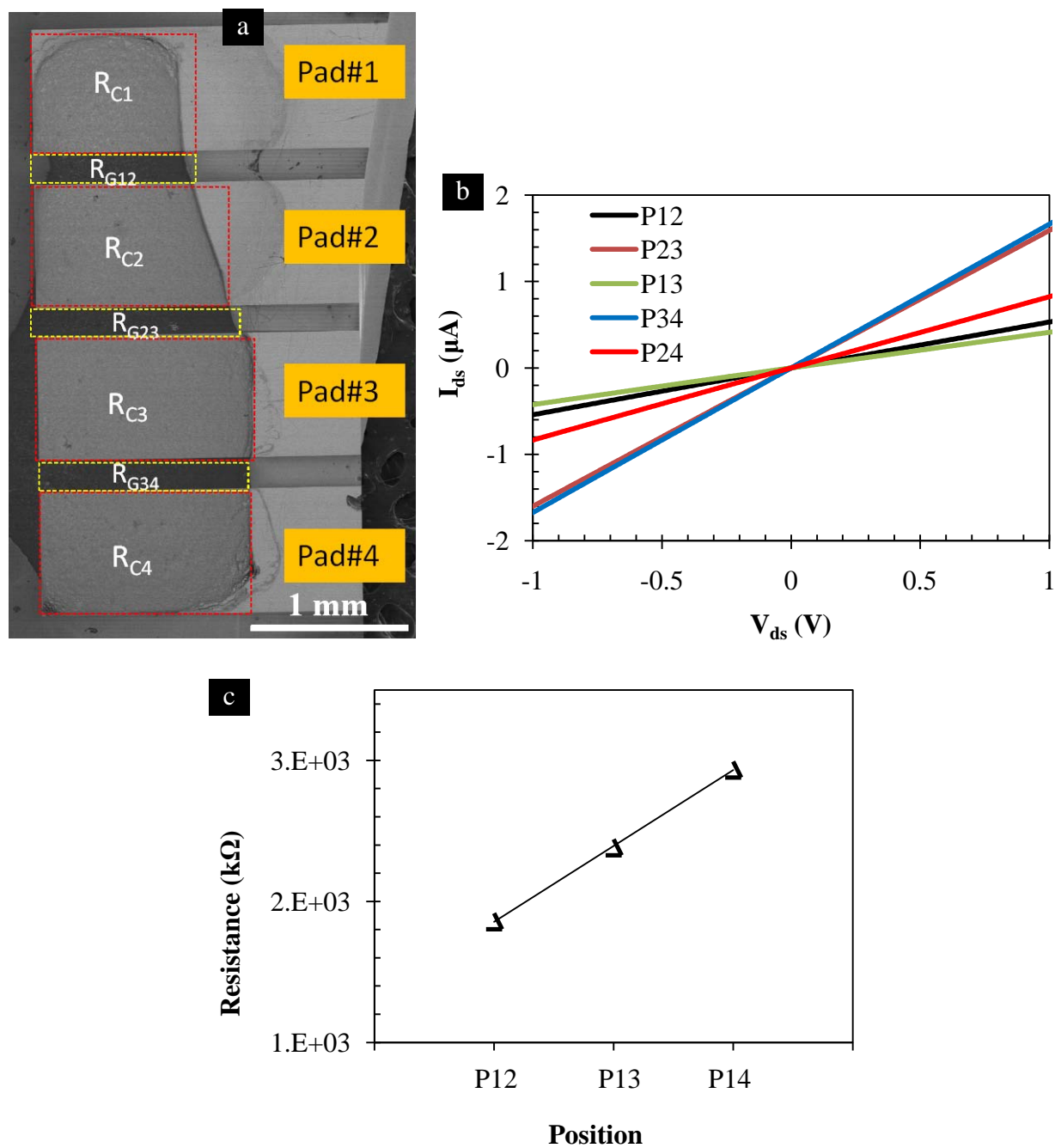


Figure S1. (a) SEM image of four Au contact pads partially covered with R-GO. (b)  $I_{ds}$ - $V_{ds}$  curves between contact pads # 1, 2, 3, and 4. (c) The resistance between a pair of Au contact pads increases quite linearly with the increasing gap distance between Au pads.

## 2. Calibration of an SWCNT sensor for NO<sub>2</sub> sensing with ( $R_a-R_g$ ) vs. $R_a$

A CNT gas sensor was fabricated by depositing a few drops of an aqueous suspension containing well-dispersed single-walled CNTs (SWCNTs) (NanoIntegris Inc.)<sup>1</sup> onto Au interdigitated electrodes. Figure S2a is an SEM image that shows SWCNTs bridging Au fingers. The transport characteristics ( $I_{ds}$ - $V_g$ ) of the SWCNT device in air are typical of a p-type semiconductor, as shown in Figure S2b.

Five cycles were carried out using the SWCNT sensor for 100ppm NO<sub>2</sub> sensing. Each cycle consisted of 5 min air blow (2lpm), 5 min 100ppm NO<sub>2</sub> exposure (2lpm), and 10 min air blow (2lpm) for device recovery. A constant, low dc drain-source current of 100 nA was maintained during the test while monitoring the drain-source voltage ( $V_{ds}$ ). Figure S2c is the dynamic response ( $V_{ds}$  vs. time) of the SWCNT device for 100ppm NO<sub>2</sub> sensing (five runs), which clearly demonstrates the drift and decline of the sensing signal sequentially. We further compared in Figure S2d the responses of the SWCNT sensor using  $R_a/R_g$  vs. time curves, which indicates the obvious decreasing of the sensing signal from one run to the next due to incomplete recovery. We then plotted the ( $R_a-R_g$ ) vs.  $R_a$  data in Figure S2e and found a very linear correlation between ( $R_a-R_g$ ) and  $R_a$ , implying that the method we proposed could be effective for overcoming the run-to-run deviation of CNT gas sensors as well.

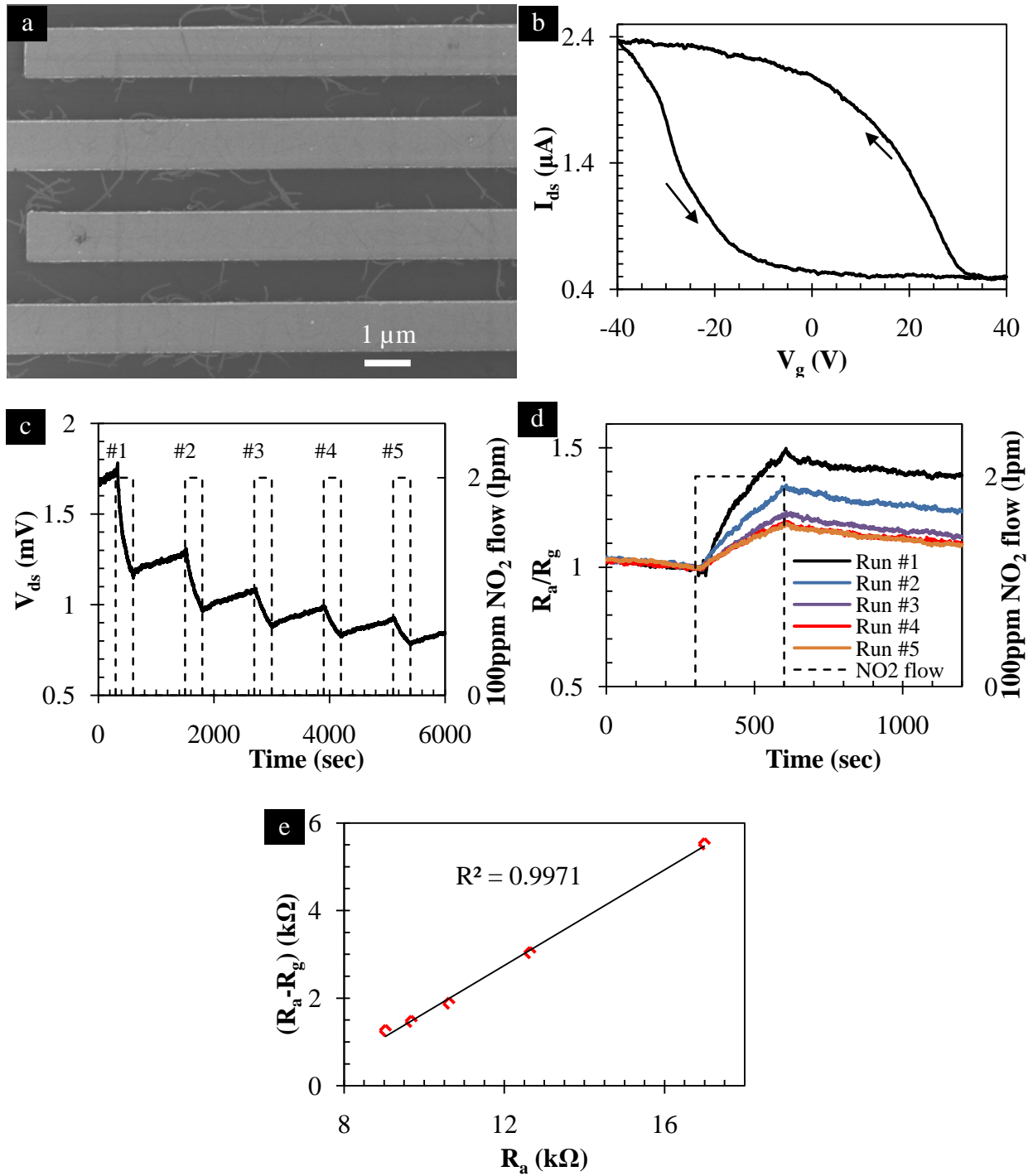


Figure S2. (a) SEM image of SWCNTs bridging Au fingers of an interdigitated electrode. (b) The transport characteristics ( $I_{ds}$ - $V_g$ ) of the SWCNT device in air, indicating p-type semiconducting behavior. (c) The dynamic response ( $V_{ds}$  vs. time) of the SWCNT device for 100ppm  $\text{NO}_2$  sensing (five runs). The  $R_a/R_g$  vs. time curves (d) and the  $(R_a - R_g)$  vs.  $R_a$  plot (e) for the five sensing runs shown in (c).

## REFERENCES

1. Arnold, M. S.; Green, A. A.; Hulvat, J. F.; Stupp, S. I.; Hersam, M. C. Sorting Carbon Nanotubes by Electronic Structure Using Density Differentiation. *Nat. Nanotechnol.* **2006**, *1*, 60-65.